



Stability field of the high- (P, T) Re_2C phase and properties of an analogous osmium carbide phase

Erick A. Juárez-Arellano^{a,d,*}, Björn Winkler^a, Alexandra Friedrich^a, Lkhamsuren Bayarjargal^a, Victor Milman^b, Jinyuan Yan^c, Simon M. Clark^c

^a Institut für Geowissenschaften, Goethe-Universität Frankfurt, Altenhöferallee 1, D-60438 Frankfurt a.M., Germany

^b Accelrys, 334 Science Park, Cambridge CB4 0WN, UK

^c ALS, Lawrence Berkeley National Laboratory, Berkeley, CA 94720, USA

^d CIICAp, The Autonomous University of the State of Morelos, Av. Universidad 1001, Cuernavaca, México, Mexico

ARTICLE INFO

Article history:

Received 13 January 2009

Received in revised form 2 March 2009

Accepted 5 March 2009

Available online 19 March 2009

Keywords:

Rhenium carbide

Osmium carbide

Synchrotron radiation

Compressibility

Diamond anvil cell

High pressures and temperatures

ABSTRACT

The formation of a hexagonal rhenium carbide phase, Re_2C , from the elements has been studied in a laser heated diamond anvil cell in a P, V range of 20–40 GPa and 1000–2000 K. No indication for the existence of cubic rhenium carbide, as suggested in the literature, or any other phase was found and Re_2C is the only phase formed in the $\text{Re}-\text{C}$ system up to around 70 GPa and 4000 K. A fit of a 3rd-order Birch–Murnaghan equation of state to the Re_2C P, V -data results in a bulk modulus of $B_0 = 405(30)$ GPa ($B' = 4.6$). The linear compressibility of Re_2C along $[001]$ (~ 500 GPa) is significantly larger than the compressibility in the (001) plane (~ 360 GPa $\parallel [100]$). Based on the observations for Re_2C , we predict the structure and elastic properties of an analogous Os_2C phase, which is, at least in the athermal limit, more stable than any other osmium carbide studied previously by density functional theory based calculations.

© 2009 Elsevier B.V. All rights reserved.

1. Introduction

In a previous study, we have provided strong experimental and theoretical evidence of the formation of a hexagonal rhenium carbide at high- (P, T) conditions up to $P_{\text{max}} = 67$ GPa and $T_{\text{max}} = 3800$ K [1]. Based on our DFT calculations, Re_2C was identified as the most likely composition of this phase and a P - T field, in which Re_2C is formed, was proposed. However, due to the restricted availability of synchrotron beam time the proposed phase diagram was sketchy. The scarcity of data also implied that our rejection of a proposed cubic polymorph with rock-salt structure was preliminary. Such a rhenium carbide polymorph had been reported by Popova et al. [2] and Popova [3], based on quenched samples synthesised at ≈ 17 GPa and 1300 K, with a lattice parameter of 4.005 Å. The gap in our earlier data in the pressure range of 20–60 GPa left open the possibility that the proposed cubic polymorph could be stable at P, T conditions not been investigated. Therefore, here we extend our earlier study to the investigation of the reaction of rhenium with carbon in the 20–60 GPa range, and to the pressure dependent behaviour of Re_2C .

As the crystal chemical behaviour of osmium is similar to that of rhenium, we extended the present investigation to an analogous Os_2C compound. Osmium carbides have long been studied, as they are thought to be outstanding candidates for ultrahard and/or ultra-stiff materials. However, the experimental basis for this discussion is slim. In fact, there are only two experimental studies in which an osmium carbide was produced [4,5], and these studies are limited to the presentation of d -spacings for an assumed WC-structure type compound. In contrast to this, there are numerous theoretical studies aimed at studying superhard or ultrastiff osmium carbides e.g. [6–10]. These studies are, however, limited to osmium carbides with a 1:1 composition, and in parts contradict each other. For example, osmium carbide with the WC-structure type is sometimes computed to be ‘mechanically and electronically’ unstable [6,7,9], while in other studies this polymorph is found to be the most stable [8,10]. The simulated X-ray powder patterns of OsC in either the WC- or NiAs-structure type bear no resemblance at all to the experimentally determined pattern [7]. We therefore thought it worthwhile to compare a hypothetical Os_2C to the existing Re_2C and predict its properties.

2. Experimental

High pressure experiments were performed at the European Synchrotron Radiation Facility (ESRF, Grenoble, beam line ID27) and at the Advanced Light Source (ALS, Berkeley, beam line 12.2.2). The experimental set-up at the ESRF has been described

* Corresponding author at: CIICAp, The Autonomous University of the State of Morelos, Av. Universidad 1001, Cuernavaca, Mexico.

E-mail address: ejuares@uaem.mx (E.A. Juárez-Arellano).

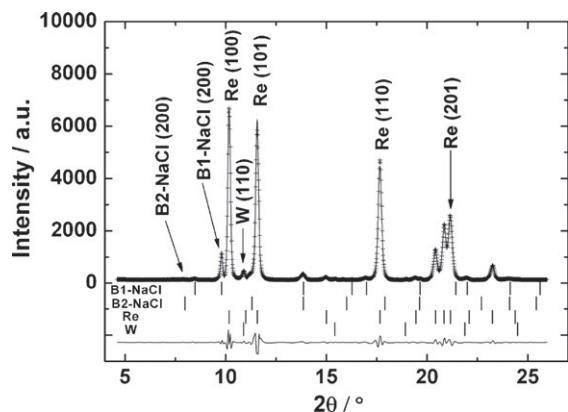


Fig. 1. Powder diffraction pattern before laser heating at 27–30 GPa, depending on which pressure scale is employed. Only rhenium, tungsten (gasket) and NaCl (pressure-transmitting medium and thermal insulation) were detected.

earlier [1]. Here, we present further data from these experiments which had not been analysed previously and which now allow to discuss the pressure dependence of Re_2C quantitatively.

For the experiments at the ALS, we used 30 keV radiation and double sided laser heating performed with fibre lasers. The experimental set-up is described in detail in [11]. We employed Boehler–Almax diamond anvil cells with conical anvils and 0.35 mm culets and effective aperture of $\approx 60^\circ$. We used tungsten gaskets, pre-indenting to 42 μm . Gasket holes with a diameter of $\approx 120 \mu\text{m}$ were drilled by a home-built laser lathe. We used NaCl as a pressure-transmitting medium and for thermal insulation. Small pieces of rhenium foil (Alpha Aesar, purity 99.99%) with a thickness of 25 μm and graphite served as starting materials. Both materials had been characterised earlier [1,12]. A ruby was loaded to allow pressure determination by the ruby fluorescence method. Due to the strong absorption of the laser radiation by the opaque samples, only moderate laser power was required to achieve bright hot spots. However, due to technical problems with the temperature determination, only approximate temperatures could be determined. Laser heating with moderate laser power (around 10–15 W per laser) led to temperatures of about 1600–2200 K in the sample. Experience shows that the optical emission of samples which react on laser heating is very variable and a more reliable temperature determination was not possible. Powder diffraction patterns were acquired with a MAR345 image plate detector. The sample-to-detector distance of 307.45 mm was determined from a LaB_6 reference sample. Counting times varied between 120 and 3600 s. Most data collection was done with a 10 $\mu\text{m} \times 10 \mu\text{m}$ beam spot. The laser spots had a diameter of about 15–30 μm . The diffraction images were processed, corrected for distortion and integrated using FIT2D [13]. Intense and well defined single-crystal diffraction spots from individual larger grains of the sample, and from the diamonds were masked manually and excluded from the integration. The background of the integrated powder diffraction patterns was extracted using the program DATLAB [14]. Le Bail fits were performed using the program FULLPROF [15] in order to obtain unit cell parameters. A linear interpolation between approximately 30 manually selected points for the background and a pseudo-Voigt profile function were used. Pressures were determined with an off-line spectrometer using the ruby fluorescence method [16] and from the known equation of state for NaCl [17,18] during the diffraction measurements. The two pressures determined independently from each other agreed typically within 2 GPa. Diffraction data were collected at different pressures without heating; at pressures of around 30 and 40 GPa prior to heating,

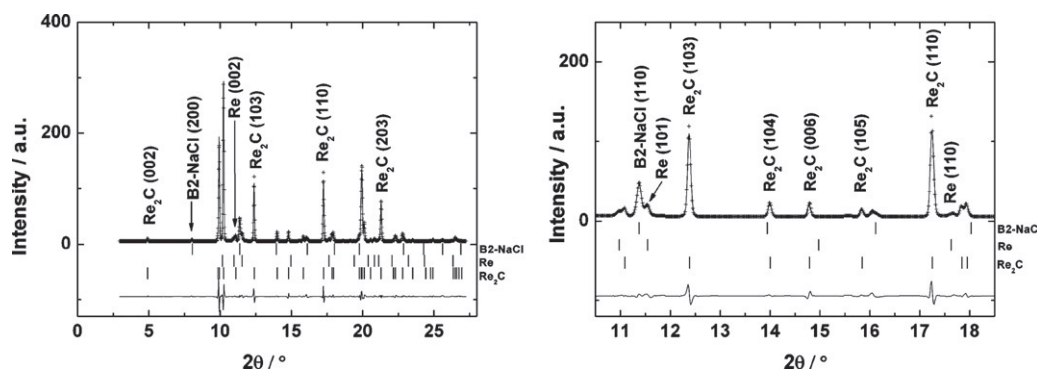


Fig. 2. Powder diffraction pattern (left: full range, right: enlargement to show the absence of any non-indexed reflections) after laser heating the sample at 40 GPa. Only Re_2C , Re and B2-NaCl (thermal insulation) were detected.

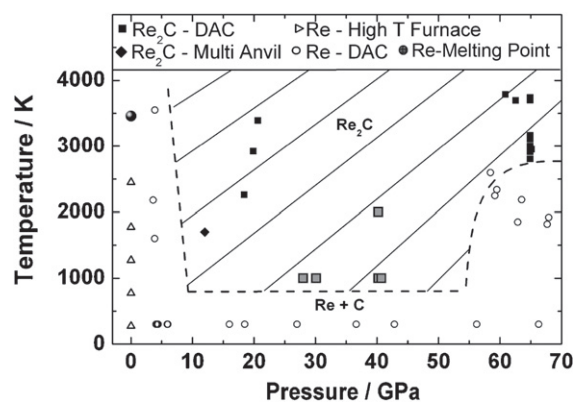


Fig. 3. Overview of the pressure–temperature range in which Re_2C can be synthesised. The hexagonal rhenium carbide Re_2C is the only phase present up to around 70 GPa and 4000 K. Grey filled squares represent results from this study while the other data points were taken from [1].

during heating and on temperature quenched samples. For each temperature run, a new sample position was selected.

3. Density functional theory

Density functional theory (DFT) calculations were performed using the CASTEP code [19]. The code is an implementation of Kohn–Sham DFT based on a plane wave basis set in conjunction with pseudopotentials. The plane-wave basis set is unbiased (as it is not atom-centered) and does not suffer from the problem of basis set superposition error unlike atom-centred basis sets. It also makes converged results straightforward to obtain in practice, as the convergence is controlled by a single adjustable parameter, the plane wave cut-off, which we set to 330 eV. All pseudopotentials were ultrasoft, and were generated using the PBE exchange–correlation functional [20] to allow for fully consistent treatment of the core and valence electrons. The rhenium atom was described with core (in parentheses) and valence regions of $([\text{Kr}]4d^{10}4f^{14})5s^25p^65d^56s^2$, the osmium was represented by $([\text{Kr}]4d^{10}4f^{14})5s^25p^65d^66s^2$ while the carbon was simply $([\text{He}])2s^22p^2$. The Brillouin-zone integrals were performed using Monkhorst–Pack grids [21] with spacings between grid points of less than 0.02 \AA^{-1} . Simultaneous geometry optimisation of unit cell and internal co-ordinates was performed so that forces were converged to 0.005 eV/\AA and the stress residual to 0.005 GPa.

In addition to a re-analysis of our earlier calculations [1] we computed the pressure dependence of the c/a -ratio of Re and Re_2C in order to be able to compare the theoretical data with experimental data, we performed a population analysis of the Re–C bonds, and we computed the structures and properties of osmium carbides.

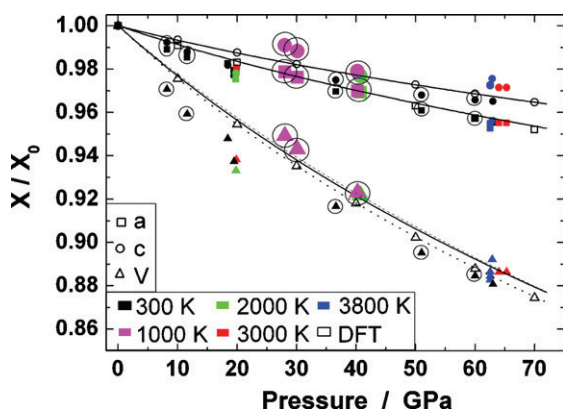


Fig. 4. Pressure dependence of the Re_2C normalised unit cell parameters. Dashed and solid lines represent 2nd- (dashed line) and 3rd-order (solid line) BM-EOS fits, respectively, to the experimental results. The DFT results (open symbols [1]) were not used for the fits. The dotted line represents a 3rd-order BM-EOS fit to the DFT results. Markers within a circle represent results from this study, while the rest were taken from [1]. Enlarged symbols represent data collected using NaCl (ALS) while the rest were collected using Ar (ESRF) as a pressure-transmitting medium.

4. Results and discussion

A typical powder diffraction pattern obtained at high pressure before any laser heating at the ALS is shown in Fig. 1. This powder diffraction pattern can be completely indexed by assigning peaks to either rhenium, tungsten (gasket) or NaCl (pressure-transmitting medium and thermal insulation). Carbon is not detectable due to its comparatively low scattering cross-section. The pressure determined by ruby fluorescence was 27(1) GPa. At this pressure, the NaCl had started to transform from the B1 ($Fm\bar{3}m$) to the B2 structure ($Pm\bar{3}m$). The pressure determined by the equations of state of B1- and B2-NaCl was ≈ 30 GPa [17,18]. The co-existence of the B1 and B2 phases and the pressures we obtained are consistent with earlier reports [22].

After laser heating the sample with low laser power (4–10 W per laser), the presence of the hexagonal Re_2C phase was detected. As mentioned above, due to technical problems an accurate temperature determination was not possible. However, typically the low laser power we used leads to temperatures of about 1000 K. The formation of the hexagonal Re_2C phase was also detected at pressures around 40 GPa at low and moderate laser power (Fig. 2). In these cases, powder diffraction patterns obtained after laser heating the sample at this pressure could be fully indexed by an assignment of peaks to either Re_2C , Re or B2-NaCl. Within our detection limits, no other phases during and after heating and on temperature quenched samples were detected. These observations reflect the high stability of the Re_2C phase, which, once it is formed, remains stable (Fig. 3).

In our previous study [1] Re_2C was identified, based on DFT calculations, as the most likely composition of the hexagonal phase, but due to the lack of data, further confirmation was required. Here, we present a more complete data set which allows an evaluation of the pressure dependence of the hexagonal unit cell parameters (Fig. 4). The scatter of the data is, in part, due to the use of different pressure scales and different pressure-transmitting media. The argon equation of state was used for the pressure determination at the ESRF, while at the ALS NaCl served as an internal standard complemented by ruby fluorescence measurements. Also, as we could only determine the temperature semi-quantitatively and thermal expansion is assumed to be small, we neglect the influence of temperature in the compressibility study, which adds further uncertainty. However, it is clear that the pressure dependence of the unit cell parameters obtained here from the experiments agrees

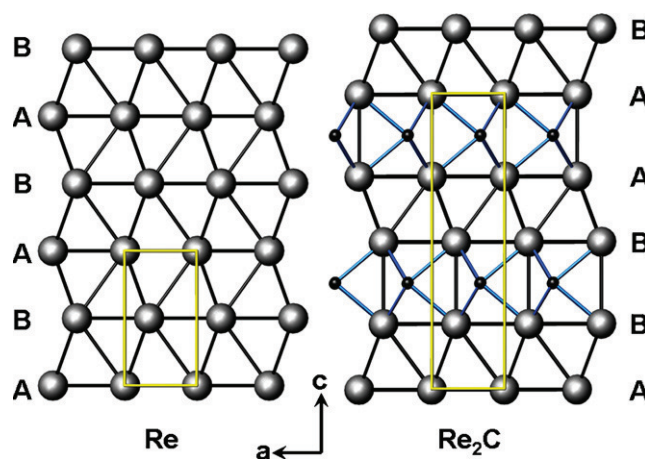


Fig. 5. Comparison between the Re and the Re_2C crystal structure. The space group symmetry of both structures is $P(6_3/m)mc$, but the carbon incorporation leads to an expansion of the a -axis from 2.803 Å for Re to 2.843 Å for Re_2C , while the c -axis is doubled and expanded from 4.461 Å for Re to 9.858 Å for Re_2C .

well with the predictions from the DFT calculations, as the EOS fitted to the experimental data describes the DFT results very well (Fig. 4). This strengthens our arguments that the composition of the hexagonal rhenium carbide phase is Re_2C , as derived from the model calculations.

It is known that transition metal carbides can be highly non-stoichiometric, and that the lattice parameters and physical properties are strongly correlated with the composition. For example, the carbon content in cubic TiC_x can vary between $1 > x > 0.5$ with corresponding lattice parameters of $a = 4.33$ Å (TiC) and $a = 4.30$ Å ($\text{TiC}_{0.5}$) [23,24]. In our earlier study [1], a series of simulations in which the amount of carbon introduced into the Re-lattice was varied were performed. From these calculations, large variations in the unit cell were observed as a function of composition ($a = 2.75$ – 2.90 Å and $c = 9.50$ – 11.00 Å). In contrast, all samples investigated at ambient pressure had lattice parameters which were, within 3σ identical, despite their very different thermal and barometric history ($a = 2.840(1)$ Å, $c = 9.85(1)$ Å, for samples quenched from 6 GPa and 1100 K [25]; $a = 2.8425(1)$ Å, $c = 9.8584(1)$ Å, for samples quenched from 12 GPa and 1700 K [1]; $a = 2.8407(1)$ Å, $c = 9.8580(6)$ Å, for samples quenched from 40 GPa and 2000 K, this study). This is a strong indication that at ambient conditions there is no significant deviation from a constant or nearly constant composition, which we have shown is likely to be Re_2C , independently of the synthesis conditions used.

4.1. Re_2C crystal structure

A comparison between the Re and the Re_2C crystal structure is shown in Fig. 5. In titanium carbide we have shown that the diffusion of carbon into an hcp structure is energetically more favourable in the basal plane than along the c -axis [12]. This seems to be the case here as well, where the carbon atoms are located on (001) planes between identical Re layers, which leads to the characteristic AABB stacking sequence of Re_2C (Fig. 5). From the DFT model, it follows that the carbon incorporation increases the Re–Re distances from 2.74–2.76 Å in the Re structure [26] to 2.78–2.85 Å in the Re_2C structure, leading to Re–C distances of ≈ 2.16 Å.

4.2. Bulk and linear compressibility

The new data obtained in the present study allowed us to investigate the pressure dependence of Re_2C . Results from fits of 2nd- and 3rd-order Birch–Murnaghan equations of state (BM-EOS) to the

Table 1

Bulk modulus and linear compressibilities obtained from fits of 2nd- and 3rd-order Birch–Murnaghan equations of state to the experimental and theoretical data of Re₂C.

	$V_0/\text{Å}^3$	B_0/GPa	B'	χ^2
Exp–2nd-order	68.4(4)	423(30)	4(fixed)	26.4
Exp–3rd-order	68.5(4)	405(30)	4.6(fixed)	21.8
DFT–3rd-order	70.75(9)	385(3)	4.6(7)	1.1
DFT ^a	70.84	378(1)	–	–
	$a_0/\text{Å}$	B_{a0}/GPa		
Exp–2nd-order	2.835(4)	372(18)	4(fixed)	9.3
Exp–3rd-order	2.836(4)	363(18)	4.26(fixed)	9.3
DFT–3rd-order	2.8478(1)	349(3)	4.26(8)	1.2
	$c_0/\text{Å}$	B_{c0}/GPa		
Exp–2nd-order	9.85(4)	521(90)	4(fixed)	17.7
Exp–3rd-order	9.86(4)	473(91)	5.50(fixed)	15.9
DFT–3rd-order	10.0731(1)	484(3)	5.50(9)	1.2

^a Derived from the elastic stiffness coefficients reported in [1].

p – V data and the pressure dependencies of the individual cell axes are summarised in Table 1. Due to the different temperatures, the use of different pressure scales and pressure-transmitting media, the numerical uncertainties of the BM-EOS parameters are large (generally < 8%, but up to 19% for B_{c0}). The slightly lower χ^2 value for the fit with a 3rd-order BM-EOS, in conjunction with the DFT results, implies that the use of a 3rd-order BM-EOS is more appropriate than the use of a pressure derivative of the bulk modulus, B' , set to 4. However, due to the availability of comparatively few data points, B' could not be independently varied during the fitting procedure. Instead, the fit was constrained using the B' value obtained from the fit to the DFT results (Table 1). Hence, we cannot associate a statistical error with it.

The bulk modulus determined experimentally in this study is very close to the bulk modulus obtained using the elastic stiffness coefficients derived from quantum mechanical calculations in our early study [1], and to the bulk modulus obtained from a BM-EOS fit to the DFT results (Table 1).

These results show that Re₂C, within a $B_0 \approx 405$ GPa is one of the least compressible carbides. Re₂C is less compressible than ZrC, HfC, NbC or TiC (with bulk moduli 207 GPa, 241 GPa, 296 GPa, 315 GPa, respectively [23]); and it has a compressibility similar to VC, TaC or WC (390 GPa, 414 GPa, 421 GPa, respectively [23]). The experimentally and theoretically determined linear compressibilities of Re₂C agree within the error bars (Fig. 4, Table 1). The c -axis is substantially less compressible than the a -axis and, hence, the c/a -ratio increases with increasing pressure (Fig. 6). For comparison, we computed the compression behaviour of pure rhenium. In contrast to Re₂C we find, in perfect agreement with experiment [27–29], that in rhenium the axial ratio c/a is virtually independent of pressure (Fig. 6). A re-analysis of our DFT data published earlier [1] showed that the Re–C bond has a significantly covalent character, as a bond population analysis gave a bond population $> 1.0 e^-/\text{Å}^3$.

5. Osmium carbide

The full geometry optimisation of hypothetical Os₂C in the Re₂C structure type under the symmetry constraints of space group $P(6_3/m)mc$ gave lattice parameters $a = 2.7777$ Å, and $c = 10.293$ Å. Os occupies the position 4f with parameters (1/3), (2/3), 0.1121. A comparison to the values for the theoretical Re₂C structure [1] shows that the c/a -ratio is larger for Os₂C (3.71) than for Re₂C (3.54). In the theoretical models the Re–C bonds ($d_{\text{Re–C}} = 2.16$ Å) are slightly longer than the Os–C bonds ($d_{\text{Os–C}} = 2.14$ Å). The bond population, which is a semi-qualitative indication for the ‘covalent

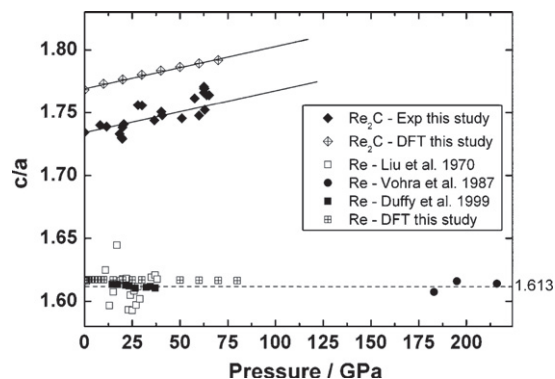


Fig. 6. Pressure dependencies of the c/a -ratios of rhenium and Re₂C. Open squares, solid circles and solid squares represent experimental data of Liu et al. [27], Vohra et al. [28] and Duffy et al. [29], respectively. Lines are guides to the eyes. The values for the length of the c -axis of Re₂C data was normalized to correspond to a cell with two Re atoms in order to facilitate a comparison with pure Re. Clearly, the DFT results have predicted the pressure-induced stiffening of the c -axis of Re₂C with respect to the a -axis very well.

character’ of the bond, is similar in both compounds ($\approx 1 e^-/\text{Å}^3$), confirming the similar crystal chemical behaviour of the two elements.

We can compute the enthalpy of formation in the athermal limit according to



and compare this to the enthalpy of formation of OsC in the WC- or NiAs-structure type. Our calculations show that the mechanical mixture of the elements is less stable than the compound by ≈ 68 kJ/(mol of osmium). This result is not very dependent on pressure, at 50 GPa the energy difference is 70 kJ/(mol of osmium). At 3000 K, which is a typical temperature at which we have synthesised Re₂C, corresponds to 360 kJ/mol. Hence, even if the entropy difference is small, as long as it favours Os₂C the reaction will proceed and Os₂C will be formed. It is worthwhile to note that a similar calculation for Re₂C also predicted the mechanical mixture to be less stable than the compound, showing that the $T\Delta S$ contribution can be large enough to lead to a free energy difference stabilising the carbide. Furthermore, given that the bonding in the various osmium carbides is not very different, we can assume a significant cancellation of errors when we compare the enthalpy of formation of Os₂C with that of OsC in the WC-structure and NiAs-structure type. In our calculations the mechanical mixture of the elements is less stable by ≈ 160 kJ/(mol of osmium) than OsC in either the WC- or NiAs-structure type at ambient pressure, and hence it seems that Os₂C would be formed if a reaction takes place in a carbon-saturated environment.

As the interest in osmium carbides is due to their potential use as ultrastiff materials, we have computed the elastic stiffness coefficients (Table 2). Os₂C has a similar bulk modulus (377(1) GPa) similar to that of Re₂C and is less compressible than any of the OsC compounds studied with DFT calculations by Guo et al. [7]. But it

Table 2

Elastic stiffness coefficients c_{ij} and bulk modulus B of Os₂C from DFT calculations. All values are given in GPa.

c_{11}	707(2)
c_{33}	724(2)
c_{44}	188(2)
c_{12}	160(2)
c_{13}	238(1)
B	377.6(7)

does not qualify as ultrastiff material, if these are taken to be those compounds which are more incompressible than diamond.

6. Conclusions

The present set of experiments complements our previous study [1] and allows us to strengthen the conclusions of some of the ideas sketched there. No indications of a cubic polymorph or another phase, such as ReC in the WC- or NiAs-structure type, suggested by Chen et al. [9] were observed in either this or in our previous study. Hexagonal Re₂C was the only phase detected up to around 70 GPa and 4000 K. From our data we are unable to unambiguously show that the cubic polymorph of rhenium carbide reported by Popova et al. [2] and Popova [3] does not exist. But what our data show is that if this phase exists it should have a very narrow stability field.

As the unit cell parameters of the rhenium carbide obtained in this and earlier studies seem to be independent of the synthesis conditions, we conclude that the composition of the hexagonal rhenium carbide phase is always close to Re₂C. We have also shown that our earlier DFT calculations correctly predicted the anisotropic compressibility of Re₂C and we have obtained an experimental bulk modulus of Re₂C which agrees within the errors with the predicted value. Clearly, what is required now are experiments to further constrain the formation conditions at comparatively low (*P*, *T*) and to provide material for the investigation of properties. Since Re₂C can be quenched, in situ studies are not required and such experiments can be performed in large volume multi-anvil presses.

We have also predicted by DFT calculations that an Os₂C phase is more stable than OsC with a WC- or NiAs-structure type and we have computed the elastic properties of this phase. We suggest that this phase can be synthesised at extreme (*P*, *T*)-conditions and are currently planning such experiments.

Acknowledgements

This research was supported by Deutsche Forschungsgemeinschaft (Project Wi-1232), in the framework of the DFG-SPP 1236. EAJA thanks the CONACyT and AF thanks the CNV-Foundation for financial support. The Advanced Light Source is supported by the Director, Office of Science, Office of Basic Energy Science, of the U.S. Department of Energy under contract DE-AC02-05CH11231. This research was partially supported by COMPRES, the Consortium for

Materials Properties Research in Earth Science under NSF Cooperative Agreement EAR 06-49658. Also, we are grateful to the ESRF for beam time and financial support.

References

- [1] E.A. Juarez-Arellano, B. Winkler, A. Friedrich, D.J. Wilson, M. Koch-Müller, K. Knorr, S.C. Vogel, J.J. Wall, H. Reiche, W. Crichton, M. Ortega-Aviles, M. Avalos-Borja, *Zeitschrift für Kristallographie* 223 (2008) 492–501.
- [2] S.V. Popova, L.N. Fomicheva, L.G. Khvostantsev, *Teoreticheskoi Fiziki* 16 (1972) 609–610.
- [3] S.V. Popova, *Acta Crystallographica A* 31 (1975) 90–99.
- [4] C.P. Kempter, M.R. Nadler, *Journal of Chemical Physics* 33 (1960) 1580–1581.
- [5] C.P. Kempter, *Journal of Chemical Physics* 41 (1964) 1515–1516.
- [6] M. Zemzemi, M. Hebbache, *International Journal of Refractory Metals & Hard Materials* 26 (2008) 61–67.
- [7] X. Guo, B. Xu, J. He, D. Yu, Z. Liu, Y. Tian, *Applied Physics Letters* 93 (2008) 041904.
- [8] Y. Liang, J. Zhao, B. Zhang, *Solid State Communications* 146 (2008) 450–453.
- [9] Z. Chen, M. Gu, C. Sun, X. Zhang, R. Liu, *Applied Physics Letters* 91 (2007) 061905.
- [10] J. Zheng, *Physical Review B* 72 (2005) 052105.
- [11] W. Caldwell, M. Kunz, R. Celestre, E.E. Domning, M.J. Walter, D. Walker, J. Glossinger, A.A. MacDowell, H.A. Padmore, R. Jeanloz, S.M. Clark, *Nuclear Instruments and Methods in Physics Research A* 582 (2007) 221–225.
- [12] B. Winkler, D.J. Wilson, S.C. Vogel, D.W. Brown, T.A. Sisneros, V. Milman, *Journal of Alloys and Compounds* 441 (2007) 374–380.
- [13] A.P. Hammersley, S.O. Svensson, M. Hanfland, A.N. Fitch, D. Hauserman, *High Pressure Research* 14 (1996) 235–248.
- [14] K. Syassen, *Datlab. Version 1.37d*, MPI/FKF Stuttgart, Germany, 2005.
- [15] J. Rodriguez-Carvajal, *Physica B* 192 (1993) 55–69.
- [16] H. Mao, P. Bell, J. Shaner, D. Steinberg, *Journal of Applied AIME Physics* 49 (1978) 3276–3283.
- [17] M. Chall, B. Winkler, P. Blaha, K. Schwarz, *Journal of Physical Chemistry B* 104 (2000) 1191–1197.
- [18] N. Sata, G. Shen, M.L. Rivers, S.R. Sutton, *Physical Review B* 65 (2002) 104114.
- [19] S.J. Clark, M.D. Segall, C.J. Pickard, P.J. Hasnip, M.J. Probert, K. Refson, M.C. Payne, *Zeitschrift fuer Kristallographie* 220 (2005) 567–570.
- [20] J.P. Perdew, K. Burke, M. Ernzerhof, *Physical Review Letters* 77 (1996) 3865–3868.
- [21] H. Monkhorst, J.D. Pack, *Physical Review B* 13 (1976) 5188–5192.
- [22] N. Nishiyama, T. Katsura, K. Funakoshi, A. Kubo, Y. Tange, Y. Sueda, S. Yokoshi, *Physical Review B* 68 (2003) 134109.
- [23] H.O. Pierson, *Handbook of Refractory Carbides*, Noyes Publication, 1996.
- [24] B. Winkler, E.A. Juarez-Arellano, A. Friedrich, L. Bayarjargal, J. Yan, S.M. Clark, *Journal of Alloys and Compounds* 478 (2009) 392–397.
- [25] S.V. Popova, L.G. Boiko, *High Temperature High Pressure* 3 (1971) 237–238.
- [26] R.J. Wasilewski, *Transactions of the Metallurgical Society of AIME* 221 (1961) 1081–1082.
- [27] L. Liu, T. Takahashi, W. Bassett, *Journal of Physics and Chemistry of Solids* 31 (1970) 1345–1351.
- [28] K.Y. Vohra, S.J. Duclos, A.L. Ruoff, *Physical Review B* 36 (1987) 9790–9792.
- [29] T. Duffy, G. Shen, D. Heinz, J. Shu, Y. Ma, H. Mao, R.J. Hemley, *Physical Review B* 60 (1999) 15063–15073.